

**An Experimental Study of  
Flame Spread Over PMMA Subject to a Water Mist**

by

Harsh P. Oke\* and Paul E. Sojka\*\*

Maurice J. Zucrow Laboratories

(formerly Thermal Sciences and Propulsion Center)

School of Mechanical Engineering

Purdue University

W. Lafayette, IN 47907-1003

Ph: (765) 494-1536 Fax: (765) 494-0530 email:sojka@ecn.purdue.edu

and

Yudaya R. Sivathanu\*\*\*

En'Urga, Inc.

1291-A Cumberland Avenue

W. Lafayette, IN 47906

Ph: (765) 497-3269 Fax: (765) 463-7004

submitted to

**Fire Safety Journal**

August 1999

1

---

\*Graduate Research Assistant

\*\*Associate Professor of Mechanical Engineering and corresponding author

\*\*Technical Director

## ABSTRACT

*An experimental study was conducted into the effect of water mist on flame spread over the solid fuel polymethyl methacrylate (PMMA). The study was carried out with two thicknesses of PMMA at four different opposing wind speeds under ambient conditions. The effect of water mist variables (inlet pressure to the atomizer, which affects the mean drop size, and flowrate through the nozzle, which affects the surface loading on the PMMA) on the flame spread rate were examined.*

*In the absence of water mist, it was found that flame spread rate decreases as the opposing wind velocity increases, and is higher for a thinner fuel than for a thicker one. In addition, the flame spread rate was found to be higher in cases where combustion took place on both sides than in analogous cases where combustion took place on only one side.*

*In the presence of water mist, the flame spread rate is a strong function of water mist loading on the unburned fuel surface; flame spread rate decreases as loading increases, with the effect more pronounced at low values of opposing wind speeds.*

## 1 INTRODUCTION

The potential role of Halons in depleting the Earth's ozone layer has motivated the world community to ban their production and phase out the existing stocks. The search for an environmentally friendly substitute has led to renewed interest in the oldest fire-fighting substance, water. Although considerable research<sup>1,2</sup> has been performed on fire suppression using water, efforts have focussed mainly on extinguishing gas-phase flames – premixed and non-premixed, co-flow and counter-flow. In contrast, the present study considers extinguishment of a flame spreading over a solid fuel using a water mist. The information provided as to the quantitative effect of an applied water mist on flame spread over a solid substance is not only important to evaluate the efficacy of water mist as a possible alternative to Halon, but is also of use in CFD modeling of fires, a subject which is gaining popularity.

Although CFD has traditionally been used to model combustors, turbines, and ductwork, it is only recently seeing increased use in the fire research community for modeling flow, temperature, and smoke in a fire scenario. Since CFD modeling requires knowledge of the heat release rates of typical materials (of which cloth, wood, and acrylic are a few) it is necessary not only to measure the heat released when such substances burn, but also to have knowledge about their fire spread rate. In a practical scenario, external factors such as ventilation due to an open window or air-conditioning would affect fire spread. Also, water sprinklers are expected to be activated and fire fighters also endeavor to bring the fire under control. The effect of such elements also needs to be factored into flame spread experiments for correct evaluation of fire spread under these conditions.

In the area of fire suppression, studies on the effect of water sprays on liquid pool fires<sup>3,4</sup> have been performed. Large-scale studies in fire suppression have also been carried

out and the chief mechanisms in fire extinguishment, namely heat extraction, oxygen displacement, and attenuation of radiation, have been identified. However no studies have been conducted on flame spread over solid combustibles in the presence of a water mist.

The present study reports flame spread rates over PMMA under countercurrent forced convection conditions in order to simulate the practical situation of a fire spreading in a draught (due to air-conditioning or an open window, for example) and exposed to a water mist (in order to simulate sprinklers). Specifically, the effect of surface water loading on flame spread rate is considered. The effect of water mist mean drop size was not investigated due to the narrow range of drop sizes employed in these experiments and because drop size measurements were not performed in the flame vicinity. This important topic may be the focus of future work.

A by-product of this study is flame spread data in the absence of water mist, which was obtained as the base case. Studies have been performed previously on the flame spread rate over PMMA subject to co-current<sup>5-7</sup> and counter-current<sup>8-11</sup> air flow. In the co-current studies there were conflicting views on the magnitude of the flame spread rate, as well as on the influence of wind speed.<sup>6-7</sup> In the counter-current flow case, the flame spread rate was shown to be dependent on not only the opposing wind speed, but also the ambient oxygen concentration.<sup>11</sup> The flame spread measurements in this work agree well with past data.<sup>11</sup>

## **2 EXPERIMENTAL APPARATUS**

The experimental apparatus consists of an aluminum-walled wind tunnel 45 cm high x 76 cm wide x 1.75 m long in which the PMMA was burned. Uniform flow in the test section was achieved by passing the flow through 6.4 mm diameter and 25 cm long

honeycomb flow straighteners. This ensured laminar, fully developed flow entering the test section. The duct had a 1 m long transition section which ended in a 30 cm diameter circular section to which a fan was mounted. Four wind speeds, viz. 0.69, 0.84, 1.21, and 1.53 m/s were obtained by varying fan motor power.

Two types of tests were run. The first set had combustion occurring only along the top surface of the PMMA and was termed “with backing”, since a 1.6 mm thick sheet of ceramic insulating paper was placed between the underside of the PMMA and the 5 mm thick aluminum plate that supported it. Water mist tests were not run for the “with backing” cases since even the lowest mass loadings extinguished the flame in less than 10 seconds. The second set had combustion occurring along both the top and bottom surfaces of the PMMA and was entitled “without backing.” In this case, the 30 cm wide x 20 cm long PMMA samples were simply supported (at the 20 cm long sides) on pieces of Unistrut<sup>®</sup> which were in turn placed on a raised platform. The gap between the underside of the PMMA and the platform was 6 cm, which exceeds the Blasius boundary layer thickness (1.4 cm) for air flowing above the support platform. As a result, free stream conditions were assumed to exist on both sides of the PMMA. All water mist tests reported here were run using “without backing” cases.

A hollow cone water spray was generated using a Variflo<sup>™</sup> simplex spill-return atomizer (Part number 33769-2) manufactured by Delavan<sup>®</sup>. The atomizer was mounted 60 cm upstream of the PMMA sample at a height of 17.5 cm (see Figure 1).

Three atomizer inlet pressures, viz. 880, 1375, and 2115 kPa, were chosen in the expectation of achieving significantly different mist mean drop sizes. A Phase/Doppler

Particle Analyzer (Aerometrics) was used separately to obtain mean drop size and drop mean velocity data.

Water flowrate through the nozzle was varied in order to alter the surface loading. The loading on the PMMA surface was obtained by determining the mass differences of pieces of absorbent paper attached to the surface of a typical sample under conditions used in the experiments.

An 8-bit 640 x 480 pixel array CCD Panasonic<sup>®</sup> camera was used to track the flame motion. The camera was connected to an Imagenation<sup>®</sup> PXC200 frame grabber. A 100 x 500 pixel image of the flame was taken every 8 seconds through use of a frequency generator-supplied trigger signal to the frame grabber.

The grabbed frames were stored in Windows BMP format. An example is shown in Figure 2. The images were then converted into ASCII format (giving the intensity values of the pixels) using Image Alchemy<sup>™</sup>, a software utility of Handmade Software, Inc.<sup>®</sup> The ASCII format was used for data reduction and analysis, as discussed below.

The flame spread rate was determined as shown in Figure 3. A frame was considered with the position of the flame (i.e., column number) in each row defined by the pixel of maximum intensity (the outermost 20 rows along each edge were ignored because flame spread is faster along the edges). The difference in flame location in a particular row between two frames separated by a known time interval yielded the flame spread rate for that row during that interval. The procedure was performed for each of the 80 rows.

Since the flame motion was usually on the order of 1 pixel between any pair of immediately adjacent frames, it was necessary to consider frames separated farther apart in time in order to observe a measurable movement of the flame and obtain an accurate spread

rate. After some trial and error it was decided that 160 seconds, i.e. 20 frames, would be an optimum length of time to get reasonable pixel movement for all flame spread rates.

The mean flame spread rate calculated for all rows was then designated as the flame spread rate for that time interval. Time-velocity traces were generated by calculating the flame spread rate at successive instants. As shown in Figure 4, such traces generally indicated a steady flame spread rate after an initial transient period.

### 3 RESULTS AND DISCUSSION

The base case result, namely flame spread over PMMA in the absence of water mist with and without backing, is shown in Figure 5. As expected, the flame spread rate for the without backing (double-sided combustion) case is higher than that for the corresponding with backing (single-sided combustion) case. This is likely due to the higher heat transfer to the unburned PMMA ahead of the flame in the without backing case.

As expected, regardless of whether backing is present or not, the flame spread rate over the thinner sample (3.2 mm) is greater than that over the thicker sample (6.4 mm). This is attributed to the fact that the former requires less heat transfer (by solid-phase and gas-phase conduction, and radiation) for raising the temperature of the unburned fuel ahead of the flame to the vaporization temperature.

Also anticipated is the flame spread rate decrease as the opposing wind velocity increases. This behavior is due to the decrease in heat transfer to the unburned PMMA via gas-phase conduction, the increased convective heat transfer from the unburned PMMA, and the lowered radiation from the flame on account of the decreased flame stand-off height and accompanying smaller view factor that occur as the opposing wind velocity rises.

The results presented in Figure 5 are about 20% greater than the findings of Fernandez-Pello *et al.*<sup>11</sup> for their 6.4 mm thick PMMA at 0.7 m/s opposed wind speed, and about 10% lower than the results of those authors at wind speeds of 0.85 m/s and 1.2 m/s. Both discrepancies are within the sum of experimental uncertainties for the two studies.

Having shown that our data in the absence of water mist is consistent with that of previous studies, we move on to consider the influence of water mist surface loading on flame spread rate. The result of flame spread over PMMA in the presence of water mist is shown in Figures 6 and 7.

Four trends can be observed when comparing data presented in Figures 6 and 7. First, we note the expected flame spread rate decrease as spray loading increases, regardless of PMMA thickness, opposing wind speed, or atomizer supply pressure. Second, the decrease in flame spread rate with an increase in water mist loading is remarkable at lower opposing wind speeds, but less noticeable as the opposing wind speed rises. Third, increasing the atomizer supply pressure heightens the effect of spray loading on flame spread rate. Finally, the thinner PMMA sample exhibits a higher flame spread rate than the thicker one.

The role of PMMA thickness is similar to that in the absence of water mist—the thinner PMMA requires less energy to sustain a flame.

The role of surface loading on flame spread can be explained as follows. There is a reduction in PMMA pyrolysis fuel ahead of the flame front due to surface cooling by the mist. As the rate of fuel vapor production decreases, the conversion of reactants to products declines with a corresponding reduction in the heat release rate. As a result, the flame spread rate decreases.

The effects of opposing wind speed and atomizer supply pressure are coupled in the water mist case. The coupling occurs through droplet evaporation within, and adjacent to, the flame zone. The data of Figures 6 and 7 are replotted in Figures 8 and 9 to better illustrate this point. The following explanation is proposed.

When the opposing wind speed is high and the atomizer supply pressure low, smaller droplets are swept over the flame zone with the result that little cooling (due to these drops) takes place and the influence of water mist is relatively low. When the opposing wind speed is low and the atomizer supply pressure is high, the drops penetrate the flame zone and evaporate within it thereby reducing the local temperature. The drop in temperature reduces the chemical reaction rate for conversion of reactants to products, which in turn results in a reduction in heat release rate. Consequently, the flame spread rate decreases. Behavior between these limiting cases occurs for intermediate values of opposing wind speed and atomizer supply pressure.

Figures 8 and 9 exhibit exactly this behavior—the influence of atomizer supply pressure is greatest for the lowest value of opposing wind speed, and decreases as opposing wind speed rises.

Our proposed explanation is supported by water mist mean drop size and drop mean velocity data acquired using an Aerometrics Phase/Doppler Particle Analyzer (P/DPA). The relationship between mean drop size and atomizer supply pressure, along with that between the vertical component of drop mean velocity and atomizer supply pressure, are shown in Figure 10.

As this figure illustrates, the drop size variation is less than  $3\ \mu\text{m}$  ( $\sim 10\%$ ) over the range of atomizer supply pressures considered. This small variation leads to only a 20%

difference in drop evaporation times, as calculated using the  $d^2$  law. The 20% difference is too small to explain the range of behavior exhibited in Figures 6 and 7 (or 8 and 9).

In contrast, Figure 10 also shows that the vertical component of the mean drop velocity ranges from less than 1 (at 880 kPa atomizer supply pressure) to nearly 3 m/s (at 2115 kPa atomizer supply pressure) over the range of loadings considered here (i.e., from 10 to 15 cc/min). As a result, drops formed by the higher atomizer supply pressure sprays are more likely to enter the flame zone, leading to a more pronounced reduction in flame spread rate.

#### 4 SUMMARY AND CONCLUSIONS

Flame spread over PMMA in the absence of water mist has been measured for two cases, with backing (single-side combustion) and without backing (double-sided combustion). As expected, the flame spread rate decreases as the opposing wind speed increases, is greater for the thinner fuel, and is higher in the case of ‘with backing’ than ‘without backing’. The difference between the present findings and those of previous investigators is within the sum of the experimental uncertainties of the studies.

Flame spread over PMMA in the presence of water mist was studied and the following behavior noted:

- Flame spread rate decreases as PMMA thickness increases. Increasing the PMMA thickness serves to reduce heat transfer to the surface ahead of the flame, thereby reducing the rate of pyrolysis and, hence, the rate of fuel-to-product conversion.

- Flame spread rate also decreases as water mist surface loading increases. Water mist also serves to reduce heat transfer to the PMMA surface ahead of the flame, with similar results.
- Flame spread rate decreases with an increase in opposing wind velocity or an increase in atomizer supply pressure. These effects are coupled—the influence of atomizer supply pressure is greatest when the opposing wind velocity is low ( $\sim 0.7$  m/s), while little effect of atomizer supply pressure is observed at the highest opposing wind velocity ( $\sim 1.5$  m/s). The coupling is thought to be due to: (i) small droplets being swept over the flame at high opposing wind speeds and low atomizer supply pressures, with the result that they do not evaporate within or near the flame zone, extract little if any energy from the flame, and therefore have only a minor effect on flame spread rate; and (ii) small droplets penetrating the flame zone at low opposing wind speeds and high atomizer supply pressures, with the result that their evaporation does extract energy from the flame and reduce flame spread rate.

## REFERENCES

1. Mawhinney, J.R., Dlugogorski, B.Z., and Kim, A.K., "A Closer Look at the Fire Extinguishing Properties of Water Mist," *Fire Safety Science - Proceedings of the Fourth International Symposium*, 1994, pp. 47-60.
2. McCaffrey, B.J., *Combustion Science Technology*, 40, 1984, pp. 107-136.
3. Braidech, M.M., Neale, J.A., Matson, A.F., and Dufour, R.E., "The Mechanism of Extinguishment of Fire by Finely Divided Water," Underwriters Laboratories Inc. for the National Board of Fire Underwriters, N.Y., 1955, pp. 7-73.
4. Rasbash, D.J., Rogowski, Z.W., and Stark G.W.V., "Mechanisms of Extinction of Liquid Fuel Fires with Water Sprays," *Combustion and Flame*, 4, 1960, pp. 223-234.
5. Loh, H.-T. and Fernandez-Pello, A.C., "A Study of the Controlling Mechanisms of Flow Assisted Flame Spread," *Twentieth Symposium (International) on Combustion*, 1984, pp. 1575-1582.
6. Apte, V.B., Bilger, R.W., Green, A.R. and Quintere, J.G., "Wind-Aided Turbulent Flame Spread and Burning Over Large-Scale Horizontal PMMA Surfaces," *Combustion and Flame*, 85, 1991, pp. 169-184.
7. Perzak, F.J. and Lazzara, C.P., "Flame Spread Over Horizontal Surfaces of Polymethylmethacrylate", *Twenty-Fourth Symposium (International) on Combustion*, 1992, 1661-1668.
8. McAlevy, R. F. III and Magee, R. S., "The Mechanism of Flame Spreading Over the Surface of Igniting Condensed-phase Materials," *Twelfth Symposium (International) on Combustion*, 1969, pp. 215-227.

9. Lastrina F.A., Magee R.S., and McAlevy III, R.F., "Flame Spread Over Fuel Beds: Solid-phase Energy Considerations," Thirteenth Symposium (International) on Combustion, 1971, pp. 935-948.
10. Fernandez-Pello, A. C., Ray, S. R., and Glassman, I., "Downward Flame Spread in an Opposed Forced Flow," Combustion Science Technology, 19, 1978, pp. 19-30.
11. Fernandez-Pello, A. C., Ray, S. R., and Glassman, I., "Flame Spread in an Opposed Forced Flow: The Effect of Ambient Oxygen Concentration," Eighteenth Symposium (International) on Combustion, 1981, pp. 579-589.

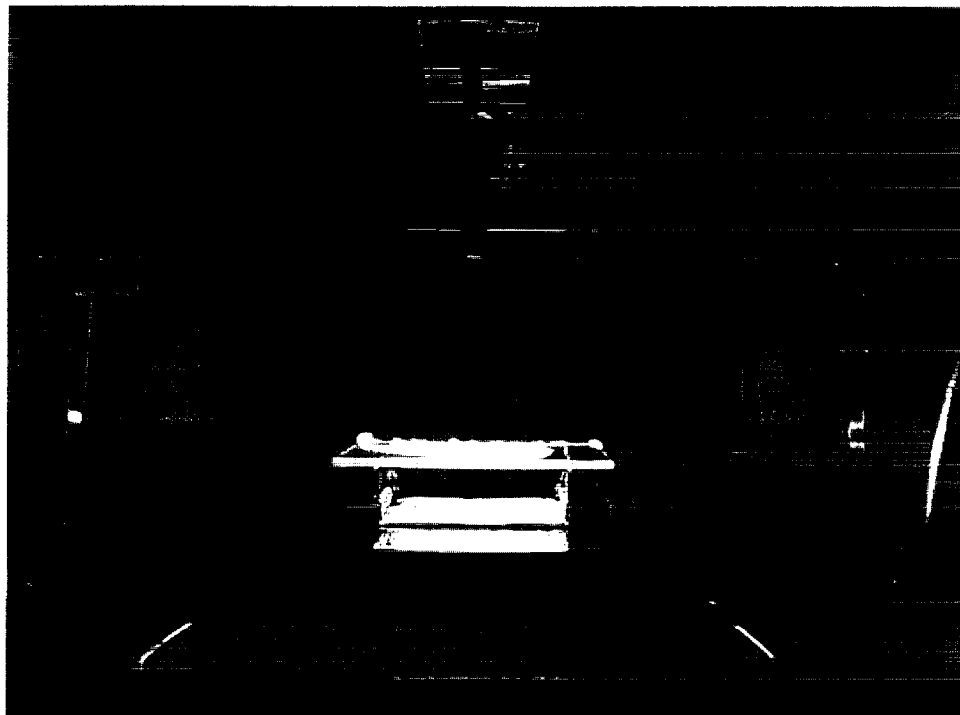


Figure 1: Flame spread over PMMA without backing under water mist

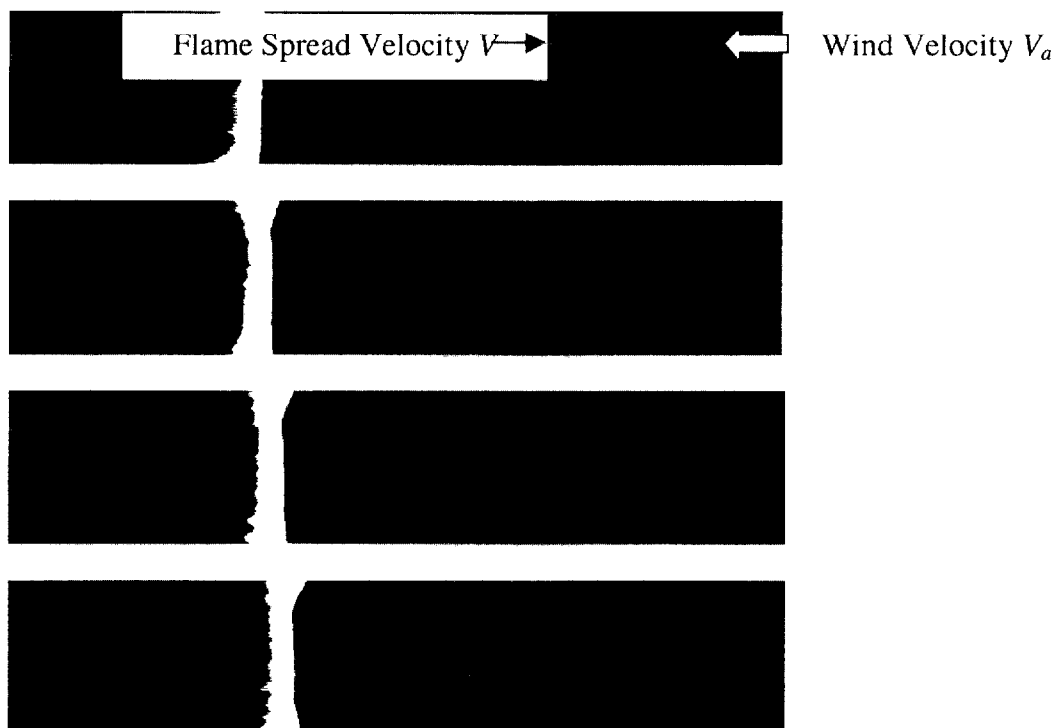
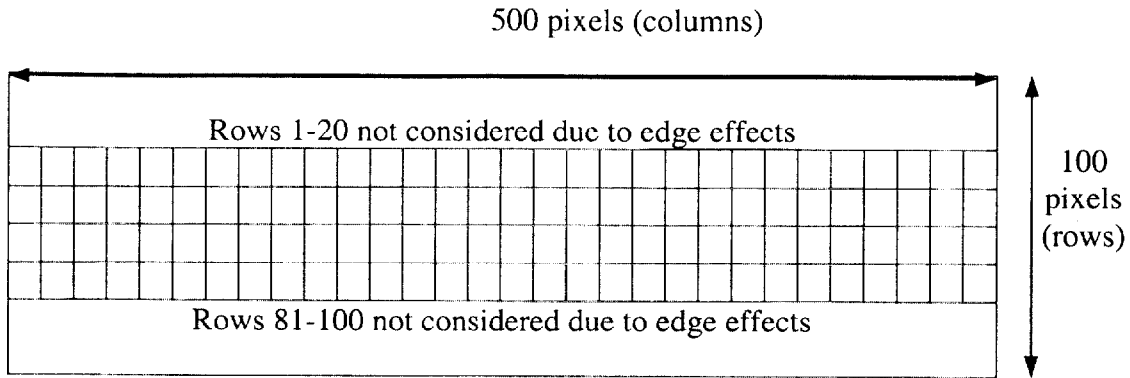


Figure 2: Typical flame spread images.



- Find the flame position (column number) in rows from 21 to 80 in frame # 1. Likewise, find the flame position (column number) in rows from 21 to 80 in all frames.
- Assuming that the test run has 99 frames, let the flame positions for rows from 21 to 80 in successive frames be as follows:

Frame # →	#1	#2	#3	...	#21	#22	#23	...	#97	#98	#99
Row 21	5	5	6	...	17	15	16	...	66	67	67
Row 22	6	6	5	...	16	16	15	...	65	68	65
Row 23	5	5	5	...	15	16	17	...	67	65	66
Row 24	4	5	6	...	15	17	17	...	66	66	68
Row 78	6	6	5	...	16	15	17	...	68	65	66
Row 79	6	4	6	...	16	17	16	...	65	67	65
Row 80	5	6	6	...	16	17	18	...	67	67	66

- Subtract frame # 1, row 21 flame position from frame # 21, row 21 flame position.  
Subtract frame # 1, row 22 flame position from frame # 21, row 22 flame position...  
Subtract frame # 1, row 80 flame position from frame # 21, row 80 flame position. This gives the flame movement in each row over the time interval between when frame # 1 and frame #21 were grabbed.
- Find the average of the flame motion and divide it by 160 seconds (time interval between 20 frames) to yield the flame spread velocity at the time frame # 1 was grabbed.
- Repeat the above two steps for frame pairs 2 and 22, 3 and 23, and so on up to frame pairs 79 and 99.  
Performing this flame spread rate calculation at successive instants yields flame spread rate versus time information, as shown in Figure 4.

Figure 3: Scheme for flame spread velocity determination

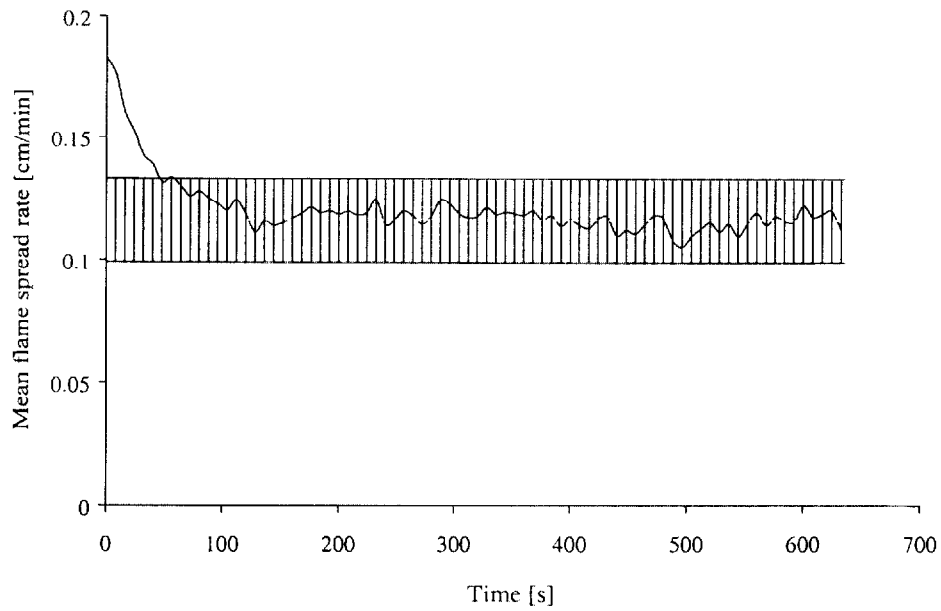


Figure 4: Typical flame spread versus time trace. Vertical bars represent experimental uncertainty. Experimental uncertainty is estimated to be less than 10% of each mean value.

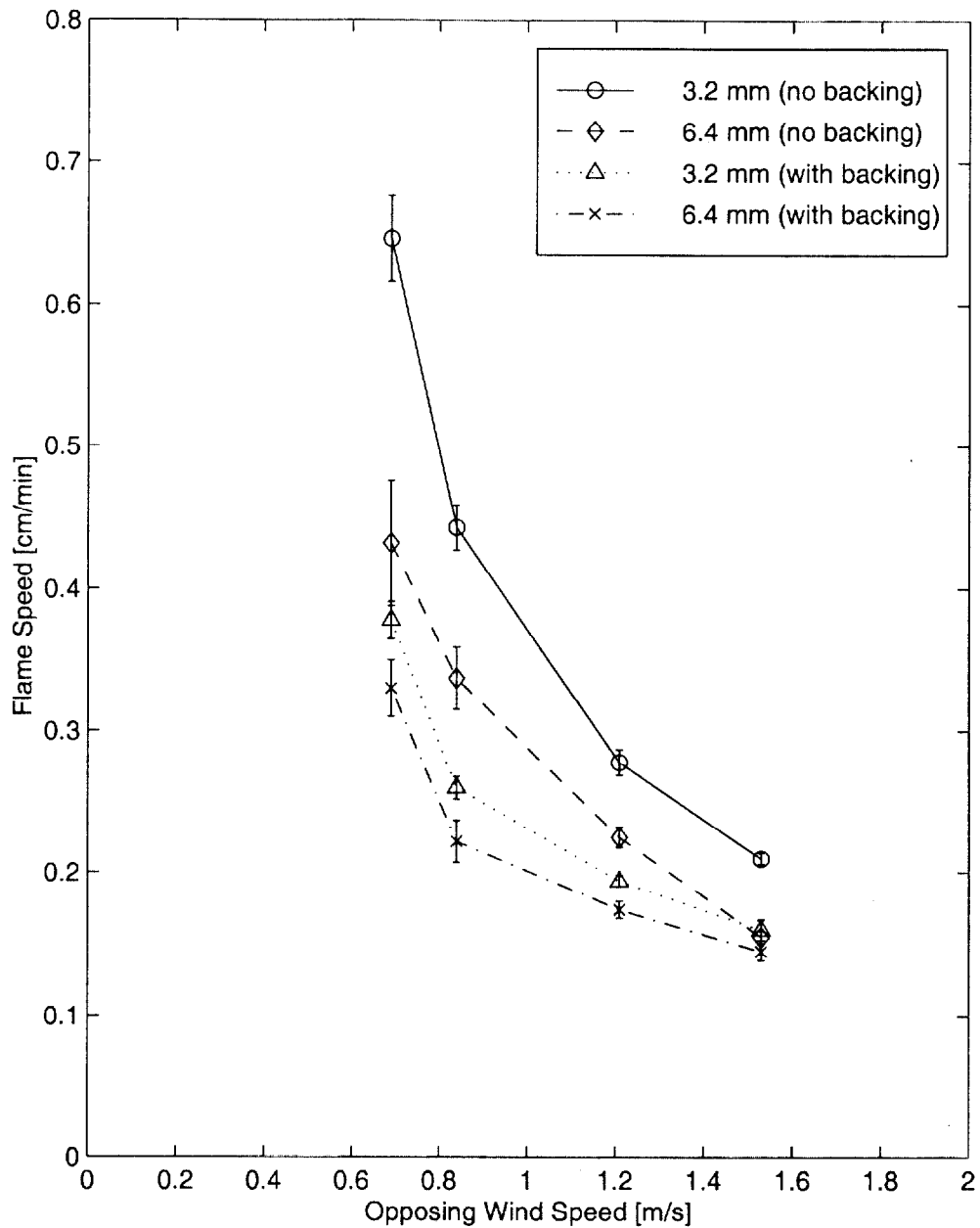


Figure 5: Flame spread in the absence of water mist. Vertical bars represent one standard deviation of statistical scatter about the mean. Experimental uncertainty is estimated to be less than 10% of each mean value.

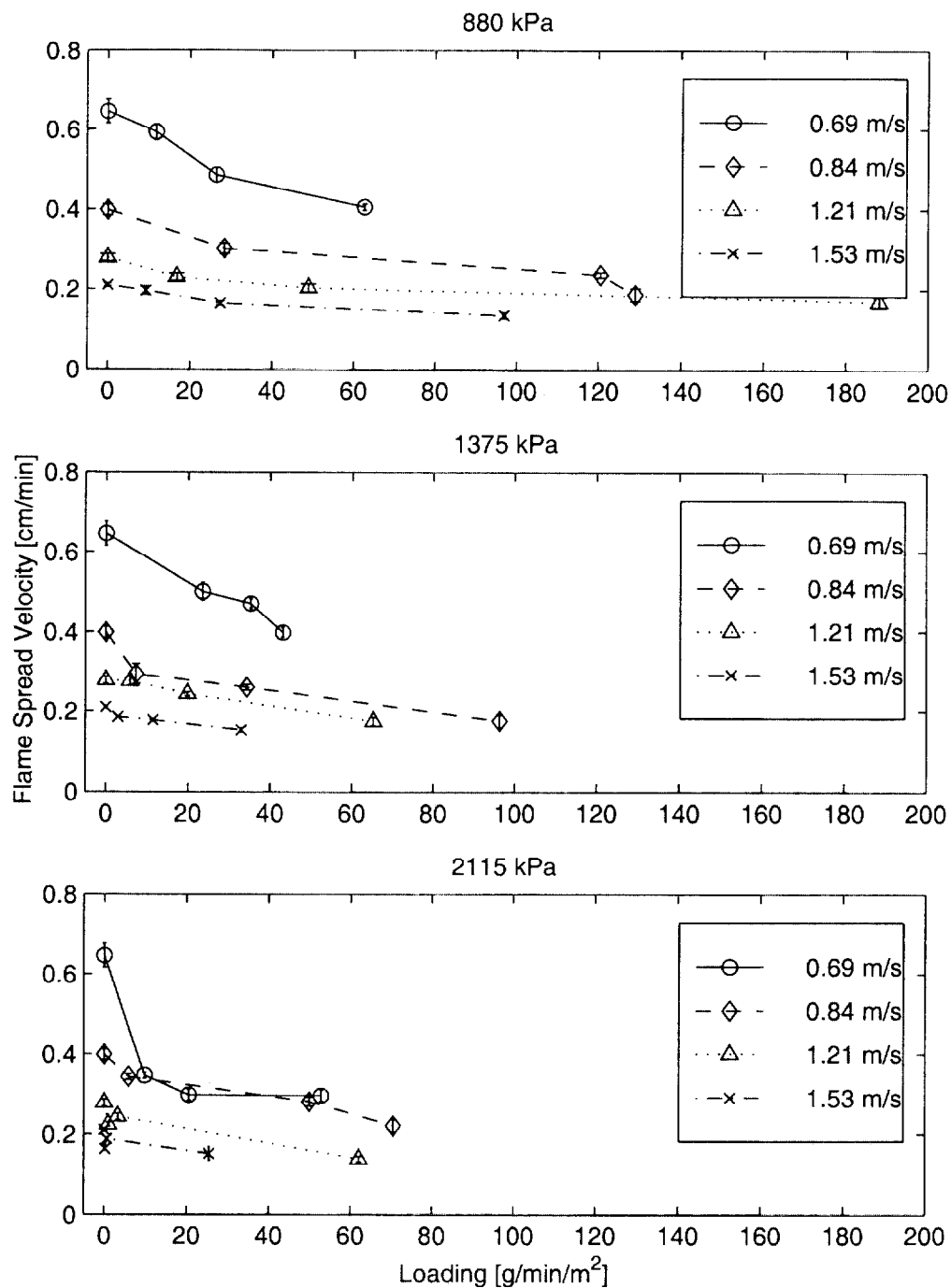


Figure 6: Flame spread as a function of surface loading for 3.2 mm thick PMMA. Vertical bars represent one standard deviation of statistical scatter about the mean. Experimental uncertainty is estimated to be less than 10% of each mean value.

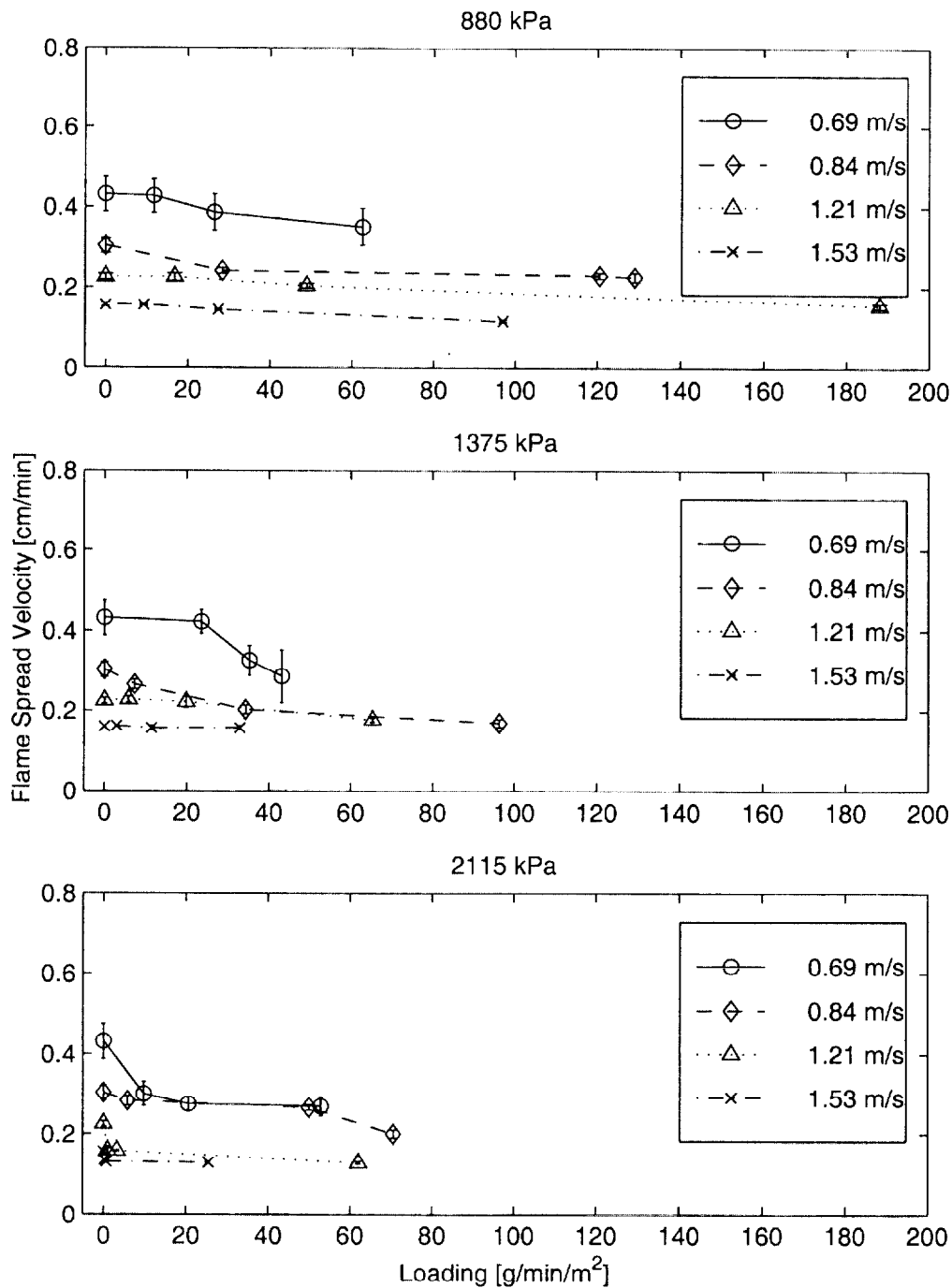


Figure 7: Flame spread as a function of surface loading for 6.4 mm thick PMMA. Vertical bars represent one standard deviation of statistical scatter about the mean. Experimental uncertainty is estimated to be less than 10% of each mean value.

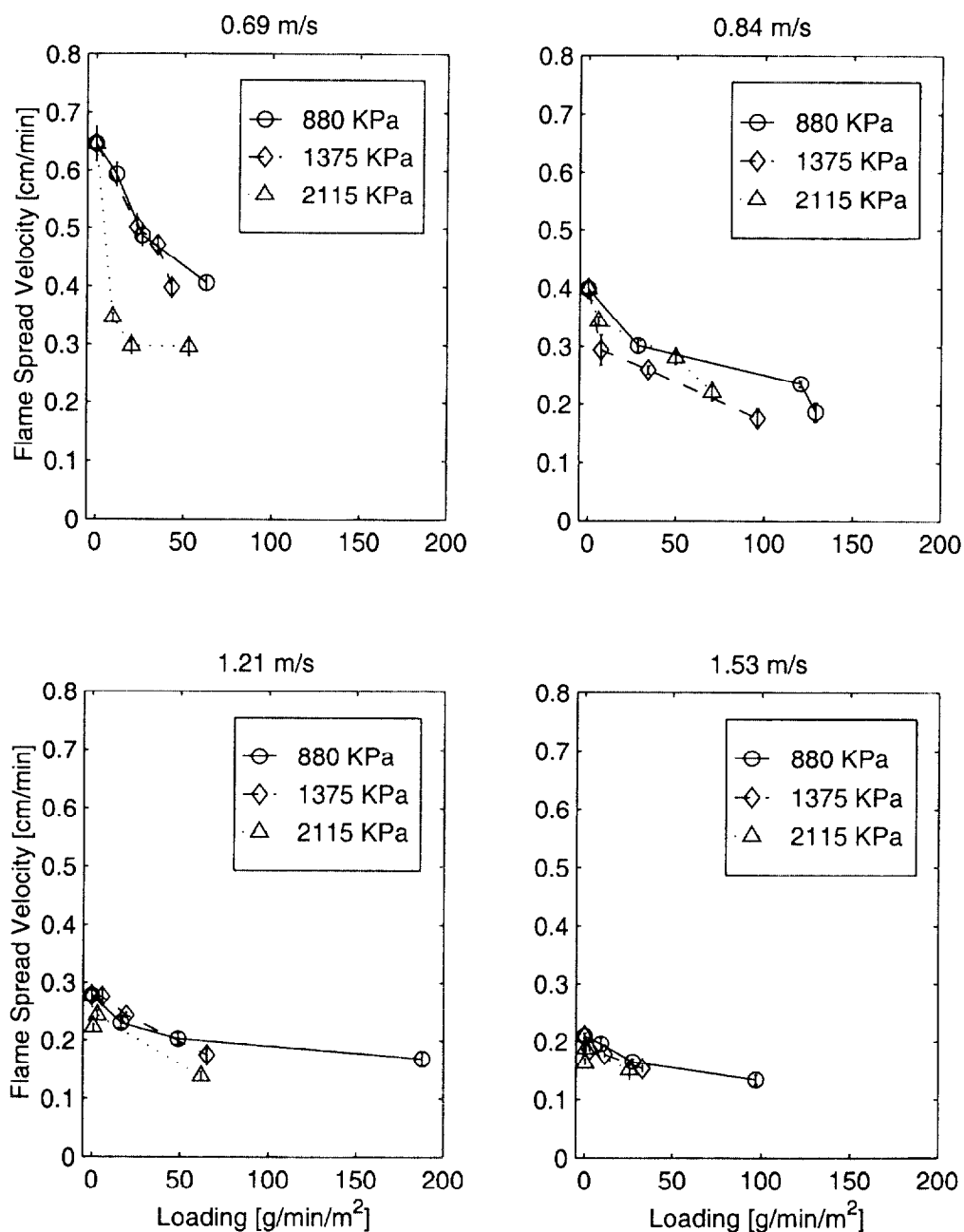


Figure 8: Flame spread rate as a function of surface loading at different atomizer inlet pressures for 3.2 mm thick PMMA. Vertical bars represent one standard deviation of statistical scatter about the mean. Experimental uncertainty is estimated to be less than 10% of each mean value.

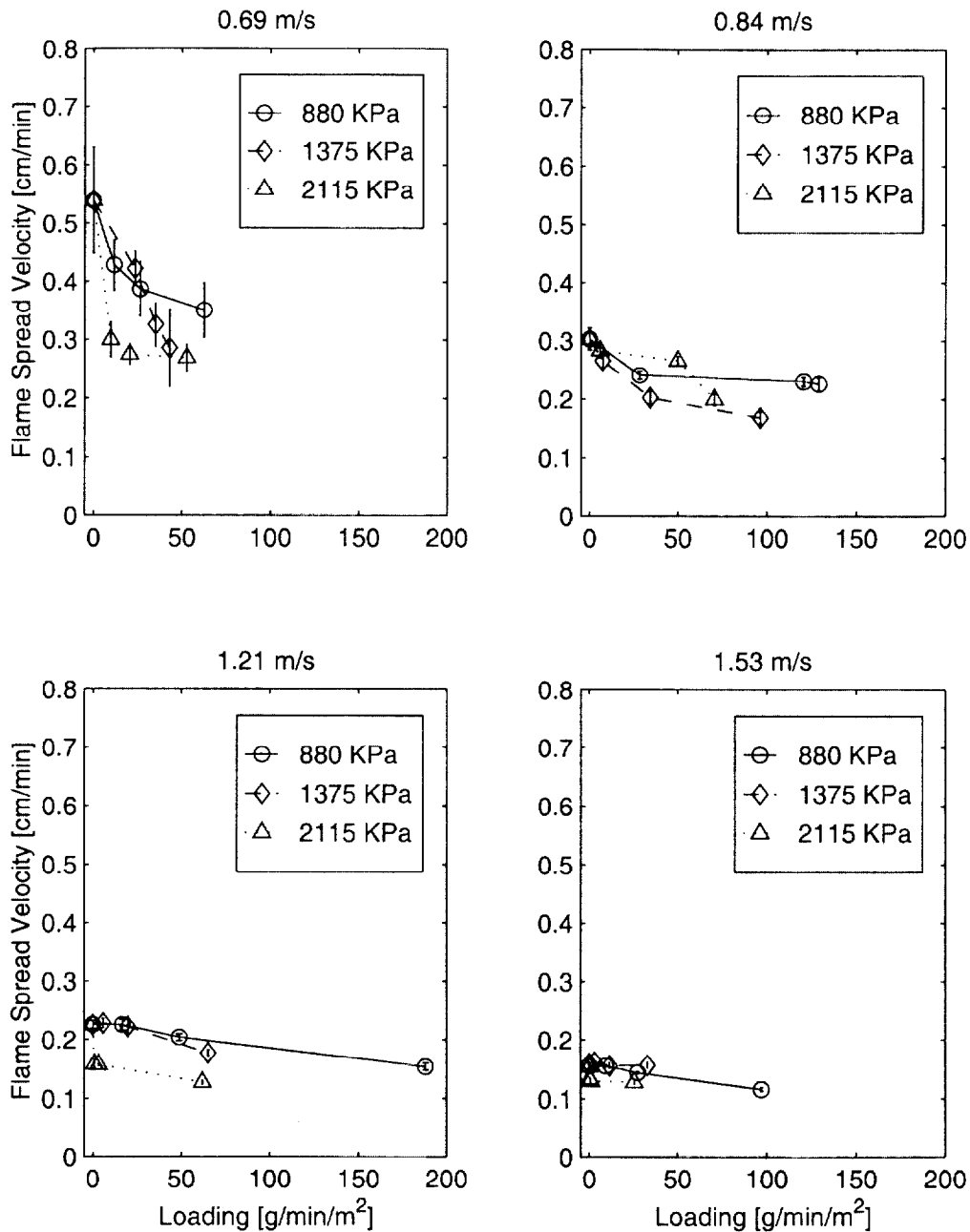


Figure 9: Flame spread rate as a function of surface loading at different atomizer inlet pressures for 6.4 mm thick PMMA. Vertical bars represent one standard deviation of statistical scatter about the mean. Experimental uncertainty is estimated to be less than 10% of each mean value.

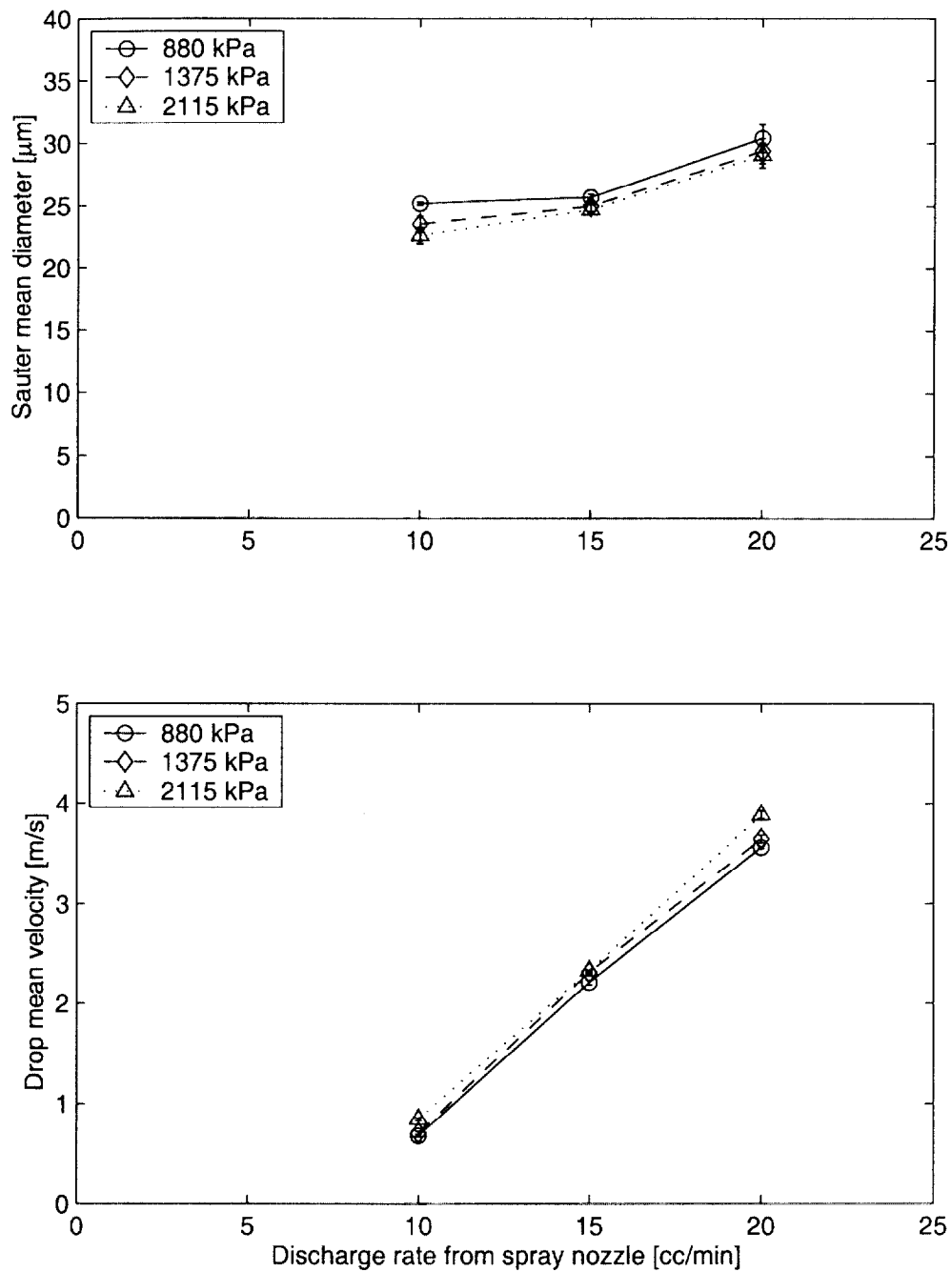


Figure 10: Mean drop size and drop mean velocity as a function of spray nozzle discharge rate.